Considerations on the thermal performances of ribbed channels by means of a novel dynamic method for hierarchical clustering

A Niro, D Fustinoni, F Vignati, P Gramazio and S Ciminà
Dipartimento di Energia, Politecnico di Milano, Milan, Italy
E-mail: alfonso.niro@polimi.it

Abstract. The investigation of ribbed surfaces for the enhancement of heat transfer in forced convection allowed to observe that different geometries may lead to comparable performances. Due to the lack of an underlying structure of the data, a novel method for data clustering is introduced here, to assess to what extent comparable performances can be achieved using different rib geometries. The clustering method is an agglomerative technique, based on the inclusion of each configuration in another ones bounding box, whose size depends dynamically on the Nusselt number and the pumping power. The method is applied to a large database experimentally obtained at ThermALab of Politecnico di Milano, in order to identify the Nusselt number and the friction factor for diverse-rib configurations in a large-aspect ratio channel with low-Reynolds flows. The clusters are determined, and the resulting families of configurations are used to assess the possible effects of the rib geometry on the thermal and fluid-dynamic performances. The clustering analysis results suggest interesting considerations.

1. Introduction

Enhancing heat transfer in forced convection has always raised a paramount interest in industrial research, as the applications range from gas-turbine blade cooling to plate-fin compact heat exchangers, including electronic components [1, 2]. On the one hand, an effective design of these devices requires large values of heat-transfer area per unit volume; on the other hand, the thermal performance is reduced when this parameter exceeds a critical value. The solution to this trade-off consists in using corrugated surfaces, including ribs or fins, which allow one to increase heat transfer without exceeding in terms of efficiency and production cost [3–6].

The large number of experimental studies performed on ribbed channels confirms their effectiveness, but also shows that the geometric factors, which condition heat transfer lead to a very large number of possible results. Moreover, it can be observed in past works that often different geometries lead to comparable performances, in terms of both thermal and hydraulic performances [7–13]. Unfortunately, experimental data show a large dispersion with respect to the controlled variables (e.g. Reynolds number, friction factor, convective heat transfer coefficient, ...) and a lack of an underlying structure. To fill this gap, the research of a criterion for the data clustering seems to be strongly desirable.

Statistical clustering is a technique used to identify the similarity among elements. It consists in classifying a number of multivariate data depending on some similarities among the members of the same set [14]. In the framework of the rib-enhanced heat transfer, each


Content from this work may be used under the terms of the Creative Commons Attribution 3.0 licence. Any further distribution of this work must maintain attribution to the author(s) and the title of the work, journal citation and DOI.
Published under licence by IOP Publishing Ltd

geometric configuration must be allocated to a set (termed *cluster*), which includes also other configurations associated to comparable thermal and fluid-dynamic performances. The so-called *agglomerative* or *top-down* methods mostly consist in iterative procedures which start with a list of the single configurations and, at each iteration, merge two elements in a cluster. After the first iteration (where no cluster has been created yet) either two configurations, or two clusters, or one configuration and one cluster, can be merged together, indiscriminately. The process then continues until all the data are merged into a unique cluster. Unfortunately, the results of these methods are not unique, as they depend on a number of parameters which must be chosen by the user, and therefore do not appear to be suitable for applications in the problem under scrutiny [15–17].

In this paper we introduce a novel method which corrects the arbitrariety of previous clustering techniques. The method, that we named "dynamic", is applied to experimental results to generate a first data clustering, and to compare overall performance data in the perspective of assessing whether comparable performances can be achieved using different rib geometries. This work is the first step to identify the most relevant geometric features in heat transfer enhancing. The database has been obtained studying the thermal characteristics of forced flow through a rectangular channel with ribs arranged in a large variety of configurations, that has been carrying on for several years at the ThermALab of Energy Department of Politecnico di Milano [18–21].

2. Features of the experimental and numerical methods

2.1. Description of the experimental setup

A large database of experimental data has been obtained studying the heat transfer characteristics of forced flow in a channel characterized by an aspect ratio of 10. The duct cross-section is 120 mm wide and 12 mm height, and the channel is operated with the lower and upper walls at fixed temperature, while the side walls are adiabatic. All the considered ribs have square cross section with different side length, pitch-to-side ratio, design and layout. Tables 1 and 2 summarize the features of the channel and ribs, respectively. Not all the possible combinations of parameters have been explored; the overall number of geometric configurations is 58, including the smooth channel, used as the reference case. Figure 1 sketches some examples of configurations.

Table 1. Main channel geometric parameters.

Channel height, h	12.0 mm
Channel length, L	880.0 mm
Channel width, w	120.0 mm
Hydraulic diameter, D_h	21.82 mm

In the images and lists of this work, the configurations are identified by means of an alphanumeric code which summarizes the ribs geometric features. The first series of symbols concerns the design: linear ribs, continuous V-shaped ribs and broken ribs are identified by the tilt angle, the letter V and the series "3D-V", respectively. In the second series there are the initial letters of the layout name. The third and the fourth series identify the pitch-to-side ratio and the side values, respectively. The smooth channel, i.e., the reference configuration, is identified by the full name. The final number, included between parentheses, is simply the run order. For example, the configuration with broken V-shaped upstream ribs, side of 2 mm and pitch-to-side ratio of 10 is termed 3D-V-up-p10-s2. Air flow rates are varied for Reynolds

Table 2. Main ribs geometric parameters. All the ribs have square section.

Rib section side, s	2 mm, 4 mm
Pitch-to-side ratio, p/s	10, 20, 40
Rib design, d	linear (tilted of 45°, 60°, 90°), continuous V-shaped, broken V-shaped. V-shaped ribs are 60°-tilted.
Ribs layout, l	aligned, staggered, crossed (for linear ribs); upstream, downstream or mixed (for continuous and broken V-shaped)

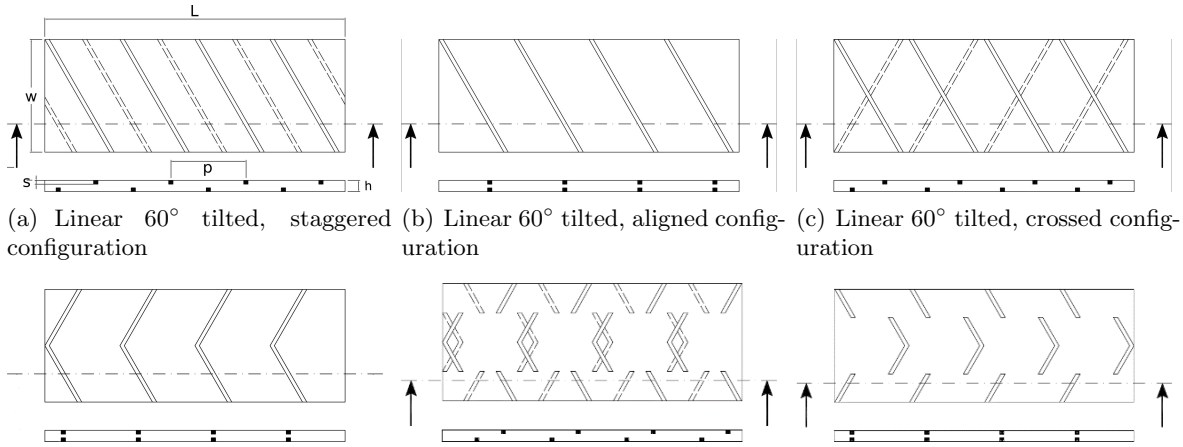

(a) Linear 60° tilted, staggered configuration

(b) Linear 60° tilted, aligned configuration

(c) Linear 60° tilted, crossed configuration

(d) Continuous V-shaped upstream, aligned configuration

(e) Broken V-shaped, mixed configuration

(f) Broken V-shaped downstream, aligned configuration

Figure 1. Sketches of some investigated configurations: (a) linear staggered, (b) linear aligned, (c) linear crossed, (d) V-shaped pointing upstream (the flow is from left to right), (e) V-shaped broken with mixed layout, (f) V-shaped broken pointing downwards. The ribs in all the depicted configurations are tilted of 60° with respect to the channel axis. The thickness and the pitch indicated in (a) are indicative.

numbers (Re) ranging between 600 and 10000. The experimental campaign moves from the consideration that, in spite of the large amount of available data, few works have focused on the study of heat exchange at low Reynolds number or for large aspect-ratio channels, albeit both appear to be very relevant to heat exchange applications [1].

The average Nusselt over the test section (Nu) is calculated as follows:

$$Nu = \frac{h\mathrm{D_h}}{k} \tag{1}$$

where $\mathrm{D_h}$ is the hydraulic diameter, and h the average convective coefficient. The latter is computed as

$$h = \frac{\dot{Q}}{A_s\,\Delta T_{ml}} = \frac{\dot{m}c_p\,(\theta_i - \theta_o)}{A_s\,[(\theta_i - \theta_o)\,/\,(\ln\theta_i/\theta_o)]} = \frac{\rho\dot{V}c_p}{A_s}\ln\frac{\theta_i}{\theta_o} \tag{2}$$

resulting in

$$Nu = \frac{\mathrm{D_h}}{k}\frac{\rho\dot{V}c_p}{A_s}\ln\frac{\theta_i}{\theta_o}. \tag{3}$$

where k the thermal conductivity of air, A_s the heated area, c_p the air constant-pressure specific heat; $\dot{Q}$ the total exchanged heat power; $\dot{m}$ and $\dot{V}$ mass and volume flow rates of air, respectively. ΔT_{ml} the logarithmic mean temperature difference, and θ_i and θ_o the wall-to-air-bulk temperature difference at the inlet and at the outlet of the channel, respectively.

The Darcy-Weisbach friction factor f is computed as follows:

$$f = \frac{\Delta p}{\rho U^2/2}\frac{\mathrm{D_h}}{\ell_{taps}} = \frac{2\Delta p A^2 \mathrm{D_h}}{\rho \dot{V}^2 \ell_{taps}} \tag{4}$$

where ΔP, U, A and ℓ_{taps} are pressure drop, cross-section area of the channel, average flow velocity and distance between the pressure taps, respectively. From the friction factor, the pumping power (PP) can be evaluated as

$$PP = \frac{\dot{m}\Delta p}{\rho}$$

Experimental results are organized in a three-dimensional space, arranged by Re, Nu and PP. Figure 2 shows a plot of Nu versus PP required to force the flow at a given Reynolds numbers. Experimental results are normalized with respect to the smooth channel data, i.e., $\mathrm{Nu_0}$ and $\mathrm{PP_0}$. Each numbered dot represents a different rib geometry: in general, adjacent numbers represent configurations with comparable geometry. Figure 2 confirms that similar thermal and hydraulic performances can be achieved when different geometries are used, and that the configurations are not organized in any evident underlying structure.

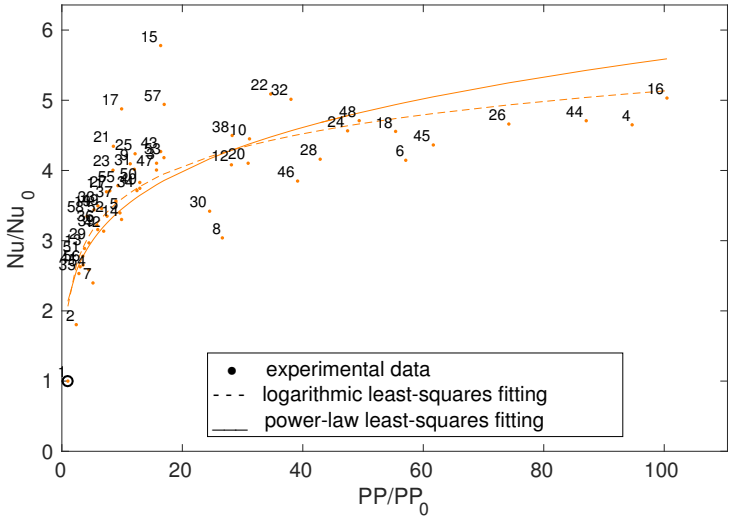

Figure 2. Experimental Nu versus PP for Re=3218. Each dot is a different geometric configuration, from 1 (smooth channel) to 58. Data are normalized with respect to the values of Nu and PP of the smooth channel. The full line and the dashed line represent fitting curves which indicate the main trend of Nu versus PP for a given Re.

2.2. Description of the clustering method

Classical agglomerative methods will be hereafter defined "static", due to their definition of the so-called *inclusion criterion* used to build the clusters. At each iteration, indeed, the distances between any two elements is computed. Then, the couple of nearest elements is selected: a new cluster is formed, which contains the two of them. The main drawback of static methods is that the clustering is quite sensitive with respect to the scaling of the data, as well as to some additional parameters which must be arbitrarily set during the tuning of the procedure. The occurrence of this problem is systematically observed in all the static clustering methods.

To overcome this limitation, the proposed clustering method is called "dynamic", and it is still an agglomerative, bottom-up technique, but it adopts a similarity criterion which disengages the results from the data scaling. This possibility comes from a proper scaling of the data which is automatically and dynamically updated during the clustering procedure. To detect the similarity between the configurations, an area of influence is identified around each configuration, whose extension is dynamically increased during the clustering procedure: if two areas of influence interact each other, then the two configurations are merged together to form a new cluster.

As a result of the specific data scaling, the dynamic clustering allows to account for the the effect of weighting of the thermo-fluid-dynamic parameters, i.e., the Nusselt number and the required pumping power, to stress the relevance of either the ribs effectiveness or the configuration efficiency. This effect can be achieved simply by modifying the aspect ratio of the area of influence of each configuration, i.e., by enlarging or shrinking it along one direction (the Nusselt number or the pumping power). Aspect ratios of 1, 5 and 10 are investigated in this work.

3. Results of the clustering analysis

For each combination of Reynolds number and aspect ratio, the hierarchical clustering is found and it is represented by means of a dendrogram. The dendrogram ordinate represents the increasing size of the area of influence, necessary to cluster the diverse configurations. This value ranges from zero (for identical configurations) to one (for the least similar configurations).

To select the configurations with a reasonable similarity degree for engineering considerations, a threshold value of 20% is selected, as it will be discussed. Therefore, the configurations with a percentage distance lesser than or equal to 20% are merged together to form groups. Figure 3 shows an example of dendrogram (in blue) obtained for Re=5353. The red line represents the threshold, i.e., the percentage distance of 20% among the configurations. Consequently, all the configurations, which are eventually merged in a branch intersecting the red line, belong to the same group because their reciprocal distance is smaller than 20%. Therefore, the groups resulting from this procedure depend on both the Reynolds number and the aspect ratio of the area of influence of the configurations. The threshold value was chosen as a result of a trade-off between two factors. On the one hand, experimental data suffer from a measurement error which, according to standard techniques [22], is less than 7% as discussed in [18–20]: hence the threshold must be larger enough to recognize real distances between configuration pairs. On the other hand, the analysis of the dendrograms suggests that threshold value larger than 20% would decrease the selectivity of the procedure. If the threshold value are too large, indeed, excessively different configurations would belong to the same group. Naturally, the validity of the proposed value of 20% is not general: with another required sensibility, the threshold value should be modified, leading to alternative groups of configurations.

It is observed that, when the aspect ratio of the influence area is larger than one, the result of the clustering is trivial. This is observed also for different values of threshold. Therefore, in the following, all the considerations concern the case on unit aspect ratio.

For every Reynolds number, the results of the described procedure are summarized by a table of size 58x58. Each row and column of the table represents one of the 58 geometric configurations. If the two configurations associated to the row-column pair of a cell belong to the same group –i.e., if their percentage distance is below 20%– the cell value is 1, otherwise it is zero. Due to its meaning, this logical value will be hereafter termed "similarity coefficient". Naturally, all the tables are symmetric and have unit values along the main diagonal.

All these tables provide complete informations but, unfortunately, they do not allow synthetic considerations. Better indications are obtained by investigating the persistence between each pair of configurations for different Reynolds numbers. To achieve this result, the tables obtained for different Reynolds numbers are combined by matrix addition: the result is a single table,

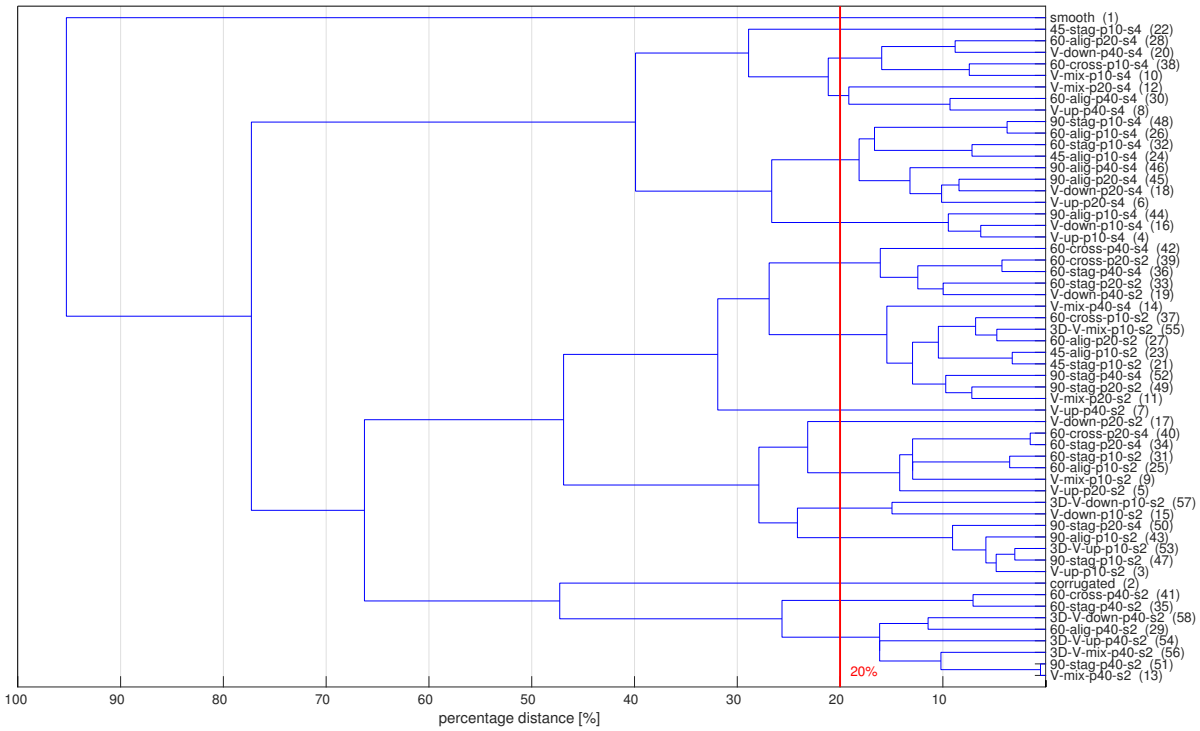

Figure 3. Dendrogram resulting from the clustering of experimental data for Re=5353 with unit aspect ratio. The horizontal red line highlights configurations with distance <20%.

termed "aggregate table", of size 58x58 which contains integer values between 0 and 8 (the same number as the investigated Reynolds values). The larger the value of a cell of the aggregate table, the more persistent the similarity between the two associated configurations. Moreover, highlighting the most persistent groupings over a range of Reynolds numbers is useful for applications with a high risk of operating in off-design conditions.

The analysis of the aggregate table suggests that configurations with very different geometric parameters systematically may group together also for diverse Reynolds. On the contrary, other configurations with similar geometry never result in comparable performances.

Figures 4(a), 4(b), 4(c) e 4(d) represent experimental data arranged in the plane Nu-PP for four Reynolds numbers, encompassing the laminar and the turbulent flow regimes in the channel. All the configurations are represented by gray dots; moreover, some specific configurations are highlighted. The configurations identified by the numbers 10 and 38 ($*$, encircled in blue) are V-mix-p10-s4 and 60-cross-p10-s4. The procedure identifies them as very similar over the whole range of Reynolds numbers (in the aggregate table their similarity coefficient is 8, i.e., equal to all the tested Re values): despite they present comparable performances, the design and layout are different, and only the rib side and pitch are the same. On the contrary, the configurations 12 and 16 (V-mix-p20-s4 and V-down-p10-s4, blue dots) result in very different performances even if they still share the value of two geometric parameters.

Interesting considerations stem from the observation of the configurations 36 and 39 (60-stag-p40-s4 and 60-cross-p20-s2, $\Diamond$, encircled in red), which present very similar performances both for laminar and turbulent flow, albeit the only common geometric parameter is the design. The opposite behavior is found in configurations 32 and 41 (60-stag-p10-s4 and 60-cross-p40-s2, red dots), which are still continuous, 60°-tilted ribs, but appear to be very distant in the Nu-PP plane for all the considered Reynolds numbers.

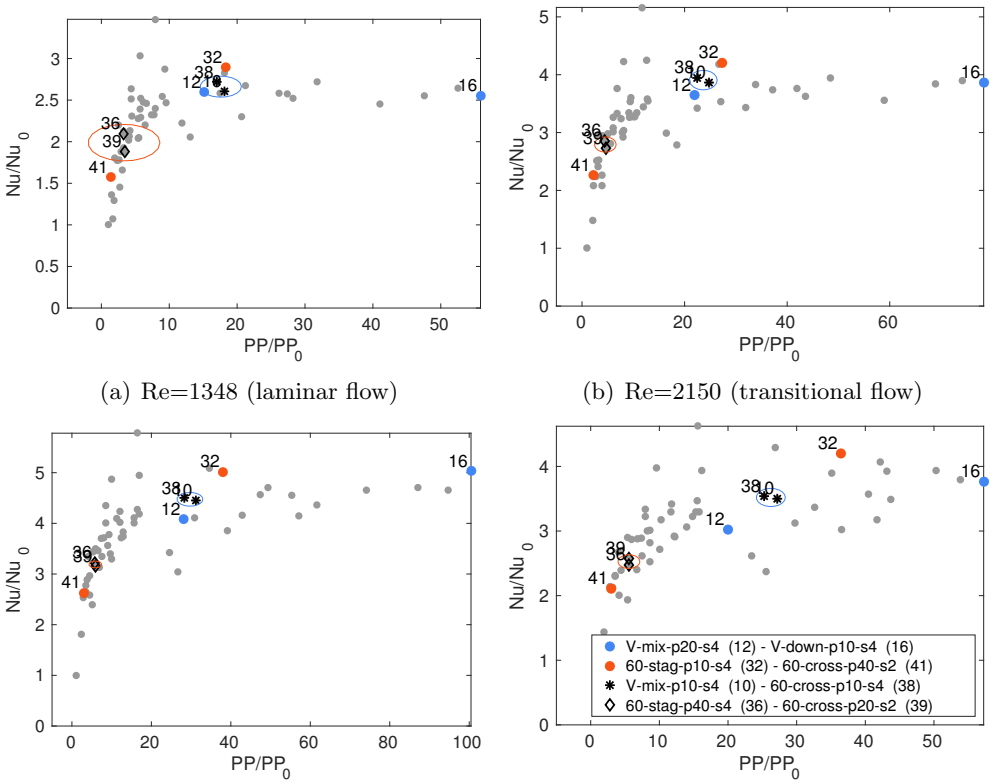

(a) Re=1348 (laminar flow)

(b) Re=2150 (transitional flow)

(c) Re=3218 (turbulent flow)

(d) Re=5353 (turbulent flow)

Figure 4. Configurations in the plane Nu-PP for different values of Reynolds number. Configurations 10 and 38 (∗) are encircled in blue in order to highlight their proximity for varying Reynolds. Configurations 12 and 16 are identified by blue dots. Similarly, configurations 36 and 39 (◊) are encircled in red, whereas the configurations 32 and 42 are represented as red dots. Gray dots indicate all the other configurations.

It is argued, therefore, that geometrically different configuration may result in similar performances due to the combined effect of the four geometric parameters. This combined effect is believed to be more relevant than each of the single parameters. However, due to the physics high complexity of the problem under scrutiny, the exact determination of the combined effect is non-trivial. Moreover, the design and layout vary only qualitatively, and therefore it is not possible to estimate the correlation between the parameters and the combined effect by means of standard statistical tools.

4. Conclusions and final remarks

A novel method was introduced for the statistical analysis of experimental data, to investigate the performances of ribs with different geometry used to enhance heat transfer in forced convection. This analysis is motivated by the empirical evidence that quite different rib geometries may often result in similar performances, despite the lack of an evident correlation between their geometry and thermal-fluid-dynamic effects.

The method was applied to study a large number of experimental data obtained during a campaign carried on for several years at the ThermALab of Energy Department of Politecnico di Milano, to identify the Nusselt number and the friction factor of low-Reynolds flows in a large-aspect ratio rectangular channel. Unlike classical clustering methods, the proposed dynamic

method disengages the clustering from the imposition of arbitrary parameters, hence resulting in unique computed families of configurations.

The analysis of the resulting clusters suggests the existence of some families of configurations which presents comparable performances. In some cases, the configurations of the same family share one or more geometric features. On the contrary, other configurations with similar geometries do not produce comparable results. Moreover, families of configurations with different geometry result in similar thermal and fluid-dynamic performances.

This first work highlights the complexity to correlate rib geometry with induced thermal and fluid-dynamic effects. Future works will focus on the underlying structure, such as the determination of the most relevant geometric parameters or of the possible existence of a unique parameter, resulting from the combined effect of geometric features, which predicts the effect of the rib geometry on the thermal and fluid-dynamic performances.

References

[1] Webb R L 1994 *Principles of enhanced heat transfer* (New York: Winley-Interscience)
[2] Gupta S, Chaube A and Verma P 2012 Review on Heat Transfer Augmentation Techniques: Application in Gas Turbine Blade Internal Cooling *J. Eng. Sci. Tech. Rev.* **1** 57–62
[3] Han J C and Park J S 1985 Heat transfer enhancement in channels with turbulence promoters *J. Eng. Gas Turb. Power* **107** 628–35
[4] Han J C, Zhang Y M and Lee C P 1991 Augmented heat transfer in square channels with parallel, crossed, and V-shaped angled ribs *J. Heat Trans.* **113** 590–96
[5] Kukreja R T, Lau S C and McMillin R D 1993 Local heat/mass transfer distribution in a square channel with full and V-shaped ribs *Int. J. Heat Mass Tran* **36** 2013–20
[6] Gao X and Sunden B 2001 Heat transfer and pressure drop measurements in rib-roughened rectangular ducts *Exp. Therm. Fluid Sci* **24** 25–34
[7] Han J C 1988 Heat transfer and friction characteristics in rectangular channel with rib turbulators *ASME J. Heat Trans.* **110** 321–28
[8] Park J S, Han J C, Huang Y, Ou S and Boyle R J 1992 Heat transfer performance comparisons of five different rectangular channels with parallel angled ribs *Int. J. Heat Mass Tran.* **35** 2891–903
[9] Han J C and Park J S 1988 Developing heat transfer in rectangular channels with rib turbolators *Int. J. Heat Mass Tran.* **31** 183–95
[10] Han J C, Ou S, Park J S and Lei C K 1989 Augmented heat transfer in rectangular channels of narrow aspect ratios with rib turbolators *Int. J. Heat Mass Tran.* **32** 1619–30
[11] Liu J, Gao J and Gao T 2012 Forced convection heat transfer of steam in a square ribbed channel *J. Mec. Sci. Tech.* **4** 1291–98
[12] Liu J, Gao J, Gao T and Shi X 2013 Heat transfer characteristics in steam-cooled rectangular channels with two opposite rib-roughened walls *App. Therm. Eng.* **50** 104–11
[13] Choi E Y, Choi Y D, Lee W S, Chung J T and Kwak J S 2013 Heat transfer augmentation using rib-dimple compound cooling technique *App. Therm. Eng.* **51** 435–41
[14] Johnson R A and Wichern D W 1992 *Applied multivariate statistical analysis* (NJ: Englewood Cliffs) vol. 4
[15] Anderberg M R 1973 *Cluster analysis for applications* (New York: Academic Press, Inc)
[16] Rand W M 1971 Objective criteria for the evaluation of clustering methods *J of the Am. Stat. Ass.* **66.336** 846–50
[17] Dav R N and Krishnapuram R 1997 Robust clustering methods: a unified view *Fuzzy Systems, IEEE Trans.* **5.2** 270–93
[18] Fustinoni D, Gramazio P, Colombo L and Niro A 2015 Heat transfer characteristics in forced convection through a rectangular channel with broken V-shaped rib roughened surface *J. of Phys.: Conf. Series* **655** 012060
[19] Fustinoni D, Gramazio P, Colombo L and Niro A 2014 Heat Transfer characteristics in forced convection through a rectangular channel with V-shaped rib roughned surfaces *15th Int. Heat Transf. Conf.*, Kyoto
[20] Fustinoni D, Gramazio P, Colombo L, Niro 2012 A First average and local heat transfer measurements on forced air-flow at low Re-numbers through a rectangular channel with ribbed surfaces *Ed. Soc. Fr. de Thermique*, Paris
[21] Fustinoni D, Niro A 2010 Experimental investigation by IR-thermography of heat transfer over rib-roughned surfaces *Heat Transf. Conf.*, Washington
[22] Moffat R J 1988 Describing the uncertainties in experimental results *Exp. Therm. Fluid Sci.* **1** 3–17